EUROPEAN SPALLATION SOURCE

Description	Technical Report
Document No	ESS-0051742
Date	August 25, 2016
Revision	3
Status	Released
Confidentiality Level	Internal

Integrity of spallation material in the target wheel during operation and accidents

	Name	Affiliation
Author	Y. Lee	European Spallation Source ERIC
Reviewers	U. Odén	European Spallation Source ERIC
	L. Coney	European Spallation Source ERIC
	J. Harborn	European Spallation Source ERIC
Approver	R. Linander	European Spallation Source ERIC

Distribution:

Contents

Document Revision History

Version	Reason for revision	Date
1	New document	2016.02.19
2	Version 2	2016.02.24
3	Updated header and footer	2016.08.25

1 Introduction

This document compiles the data on the material properties of tungsten, which is relevant to SSM application.

2 Material Selection for the spallation material

In order to maximize the neutron yield for given proton beam energy, it is required to keep the spallation volume of the target in which proton impinges as small as possible. This requirement is satisfied by choosing the target material that has a high atomic number with a high mass density. At ESS, pure tungsten has been selected as the affordable high density target material. Compared to other tungsten alloys such as densimet 18 and tungsten with 10% rhenium impurity, the pure tungsten has better residual ductilities under neutron irradiations showing the lowest degree of irradiation-induced microstructural disintegration [1]. The higher thermal conductivity of the pure tungsten than those of the compared tungsten and tantalum based alloys in Ref. [2] will result in smaller temperature gradients in the spallation volume.

Specifically, rolled and annealed tungsten will be used for the target wheel. It shows a high mass density and superior mechanical strength compared to sinterred and HIP'ed and forged tungsten [3]. The rolled and annealed tungsten shows a large grain size, as the rolling is performed at high temperatures above the recrystalization temperature of tungsten. The grains are stretched along the rolled direction with typical grain size about 400 × 50 μm minimum, as shown in Fig. 1.

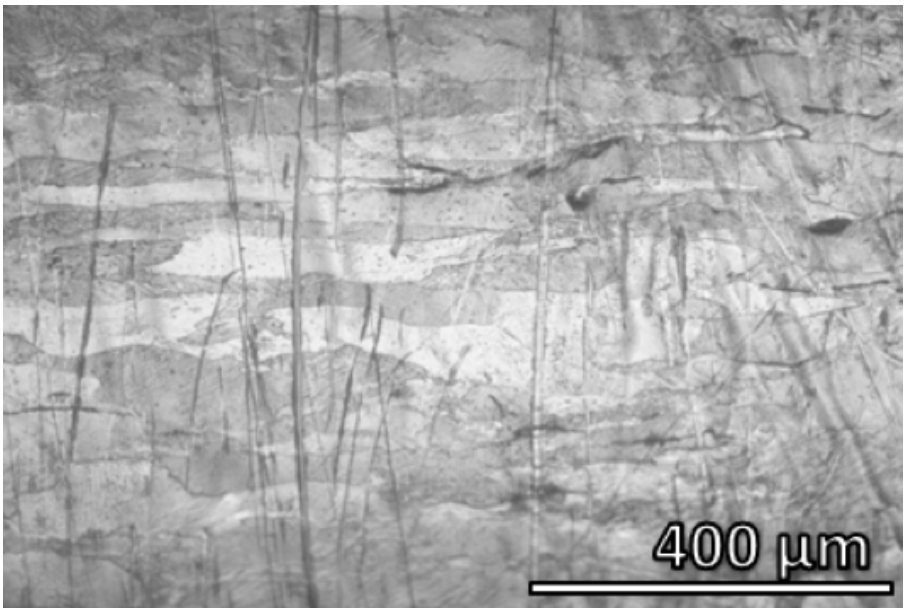

Figure 1: Microscopic image of the polished rolled tungsten specimen before fatigue test [3].

3 Chemical Composition

The chemical composition of tungsten according to technical specification of PLANSEE SE is listed in Table 1 which is taken from Ref. [4]. As PLANSEE SE is a sole tungsten provider in Europe, which can provide large volume of tungsten needed for the ESS target manufacturing, the typical analyses data provided in the table will serve as the baseline chemical composition to be used for the activation calculations needed for the handling and disposal of the ESS target, until the final vendor is selected.

4 Oxidation

Though the tungsten will be placed in "pure" helium flow, a small oxygen impurity might cause surface oxidation of the tungsten for a long time operation. For this reason, the effect of small amounts of oxygen (0.5 to 510 Pa) and water vapour (650 to 800 Pa) in helium gas on the oxidation of tungsten in the temperature interval 200 °C to 900 °C has been investigated [5]. Simultaneous thermal analysis (STA) was used to examine foil specimens over a longer period of time (48h) at 500 °C and 550 °C. The results showed that even a small

Impurity Elements	Guaranteed analyses max. [μg/g]	Guaranteed analyses max. [appm]	Typical analyses max. [μg/g]	Typical analyses max. [appm]
Ag	5	8.52	5	8.52
Al	15	102.21	10	68.14
As	5	12.27	1	2.45
Ba	10	13.39	2	2.68
C	30	459.22	15	229.61
Ca	10	45.87	5	22.93
Cd	10	16.35	1	1.64
Co	10	31.20	5	15.60
Cr	10	35.35	10	35.35
Cu	10	28.93	5	14.46
Fe	30	98.77	15	49.38
H	5	910.10	1	182.02
K	10	47.02	5	23.51
Mg	5	37.81	5	37.81
Mn	5	16.73	5	16.73
Mo	100	191.62	20	38.32
N	10	131.22	5	65.61
Na	10	79.97	5	39.98
Nb	10	19.79	5	9.89
Ni	20	62.65	5	15.66
O	30	344.70	5	57.45
P	50	296.80	20	118.72
Pb	10	8.87	5	4.44
S	5	28.66	2	11.46
Si	20	130.89	10	65.45
Ta	10	10.16	5	5.08
Ti	10	38.40	2	7.68
Zn	5	14.06	5	14.06
Zr	10	20.15	2	4.03

Table 1: The chemical composition of pure tungsten according to technical specification of PLANSEE SE taken from Ref. [4]. The typical analyses data provided in the table will serve as the baseline chemical composition to be used for the activation calculations, until the final vendor is selected.

oxygen impurity of 5 ppm in the protective gas is enough to oxidize tungsten, even at temperatures as low as 400 °C. The transition temperature from the parabolic kinetics (associated with the formation of a protective oxide scale) to the linear kinetics (associated with non-protective oxidation) in tungsten is known to be in the range between 500 °C and 550 °C [6]. For this reason, it is advised to keep the operational temperature below 500 °C to avoid any erosion of the tungsten slab due to the up to 200 m/s fast helium flow.

The threshold temperature for the tungsten oxide volatilisation is known to be above 700 °C and below 800 °C [7] in the presencee of water vapour. The volatilisation of tungsten leads to elevated release level of volatile radionuclides from the tungsten volume, which results in higher environmental impacts. For the accidental cases where the first two barriers (the target vessel and the monolith vessel) lose their confinement function and the tungsten volume is exposed to air or steam, it is advised to keep the tungsten temperature below 700 °C.

At above 800 °C, the exothermic heat from the oxidation reaction is large enough to drive the temperature of tungsten further upwards, whch could initiate a run away process leading to a total volatilisation of a tungsten mass, as can be shown below.

The enthalpies of chemical substances involved in Tungsten oxidation processes are listed in Table 2.

Formula	**State of Matter**	**Enthalpy [kJ/mol]**
W	Solid	0.0
O_2	Gas	0.0
WO_2	Solid	-589.69296
WO_3	Solid	-842.90864

Table 2: Standard thermodynamic values for relevant materials.

The enthalpy change for Tungsten oxidation processes are given by:

$$W[s] + O_2 \rightarrow WO_2[s] \qquad \Delta H = -589.7\text{kJ/W-mol} \tag{1}$$

$$W[s] + \frac{3}{2}O_2 \rightarrow WO_3[s] \qquad \Delta H = -842.9\text{kJ/W-mol} \tag{2}$$

These reactions result in mass changes of solid:

$$W[s] + O_2 \rightarrow WO_2[s] \qquad \Delta m = m_{\mathrm{WO_2}} - m_{\mathrm{W}} = 32\,\text{g/W-mol} \tag{3}$$

$$W[s] + \frac{3}{2}O_2 \rightarrow WO_3[s] \qquad \Delta m = m_{\mathrm{WO_3}} - m_{\mathrm{W}} = 48\,\text{g/W-mol} \tag{4}$$

The generation of exothermic heat $Q_{\mathrm{exothermic}}$ is given by:

$$Q_{\mathrm{exothermic}}\,[\mathrm{W/m^2}] = \text{Oxidation Rate}\,[\text{W-mol/m}^2\text{/s}] \times \Delta H\,[\text{J/W-mol}]. \tag{5}$$

The oxidation rate can be deduced from mass change rate during surface oxidation. The transient mass change per unit surface area in air are shown in Fig. 2, at different temperatures. From Fig. 2, the empirical value of the oxidation rate of Tungsten in air above 600 °C is in the order of $\mathcal{O}(1)$ mg/cm^2/h. The mass change rate 1.0 mg/cm^2/h is approximately equivalent to Tungsten oxidation rates given below.

$$1\,\mathrm{mg/cm^2/h} \quad \Leftrightarrow \quad 8.68 \cdot 10^{-5}[\text{W-mol/m}^2\text{/s}] \quad \text{for} \quad W[s] + O_2 \rightarrow WO_2[s] \tag{6}$$

$$\Leftrightarrow \quad 5.79 \cdot 10^{-5}[\text{W-mol/m}^2\text{/s}] \quad \text{for} \quad W[s] + \frac{3}{2}O_2 \rightarrow WO_3[s] \tag{7}$$

From Eqs. (5), (6) and (7), one obtains

$$Q_{\mathrm{exothermic}} = 5.12 \cdot 10^1\ [\mathrm{W/m^2}] \quad \text{for} \quad W[s] + O_2 \rightarrow WO_2[s] \tag{8}$$

$$Q_{\mathrm{exothermic}} = 4.88 \cdot 10^1\ [\mathrm{W/m^2}] \quad \text{for} \quad W[s] + \frac{3}{2}O_2 \rightarrow WO_3[s] \tag{9}$$

for the normalized mass change rate 1.0 mg/cm^2/h.

Consider the Tungsten slab with dimension $30 \times 10 \times 80$ mm^3. This represents a typical size tungsten blocks that comprise target volume in Technical Design Report. The total surface area of tungsten that is under oxidation process in 36 target sectors is about 50 m^2. For the oxidized tungsten target with 50 m^2 surface area, we estimate the exothermic heat generation rate to be given by

$$Q_{\mathrm{TungstenTarget}} = 2.56\,[\mathrm{kW}] \quad \text{for} \quad W[s] + O_2 \rightarrow WO_2[s] \tag{10}$$

$$= 2.44\,[\mathrm{kW}] \quad \text{for} \quad W[s] + \frac{3}{2}O_2 \rightarrow WO_3[s] \tag{11}$$

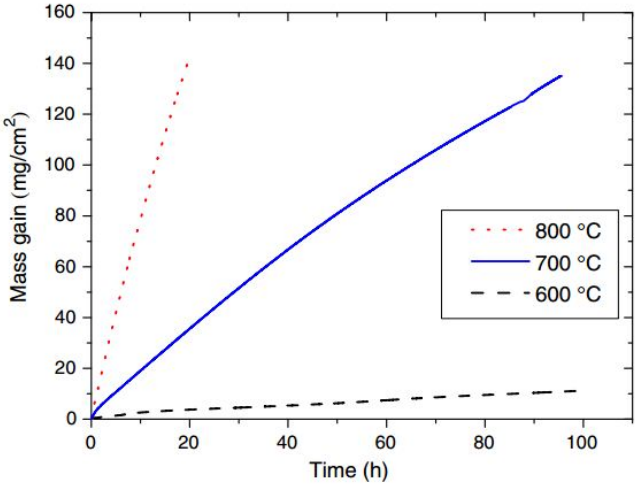

Fig. 2. Mass gain curves of pure tungsten in dry air between 600 and 800 °C.

Figure 2: The transient mass change per unit surface area in dry air [8].

for the normalized mass change rate 1.0 mg/cm^2/h.

From Fig. 2 and Eqs. (10) and (11), we can roughly summarize the exothermic heat generation rate from the ESS Tungsten slabs in the target wheel as in Table 3. The assumption taken here is that the Tungsten slabs are exposed to air and the decay heat drives the oxidation reactions at high temperatures. Furthermore, the enthalpy change due to volatilization of WO_3 is not taken into account.

Temperature [°C]	**Approx. Mass Change Rate** [mg/cm^2/h]	**Reaction formula**	**Exoth. Heat from Target** [kW]
600	0.1	$W[s] + O_2 \rightarrow WO_2[s]$	0.3
600	0.1	$W[s] + \frac{3}{2}O_2 \rightarrow WO_3[s]$	0.2
700	1.4	$W[s] + O_2 \rightarrow WO_2[s]$	3.6
700	1.4	$W[s] + \frac{3}{2}O_2 \rightarrow WO_3[s]$	3.4
800	7.0	$W[s] + O_2 \rightarrow WO_2[s]$	17.9
800	7.0	$W[s] + \frac{3}{2}O_2 \rightarrow WO_3[s]$	17.1

Table 3: The appoximate exothermic heat generation rate in Tungsten Target.

Note that the generated exothermic heat reaches $\mathcal{O}(10)$ kW at 800 °C, which is of the same order of magnitudes of the decay heat that is calculated to be 40 kW.

For this reason, the tungsten pieces must be kept below 700 °C within the site boundary of ESS, in order to avoid a harzardous situation.

5 Hydrogen generation from steam reaction

In the presence of steam at high temperatures, tungsten reacts with steam to generate hydrogen, and the hydrogen concentration must be maintained below explosive levels. The ignition point of the hydrogen contents in air is 3.6 mol-%. Smolik et al studied effects of steam pressure between $2.8{\cdot}10^4$ and $8.5{\cdot}10^4$ Pa and gas velocity between 0.011 and 0.063 m/s [9]. The observed empircal formula for the hydrogen production rate at STP is

$$\dot{V}_{H_2} = 1.02 \cdot 10^5 \times P^{0.78} \times |\overrightarrow{v}|^{0.56} \times \exp\left[-1.672 \cdot 10^4/T\right], \tag{12}$$

where the hydrogen generation rate $\dot{V}_{H_2}$ in liter/m^2/s, the pressure P is in atm and the velocity of inlet steam flow $|\overrightarrow{v}|$ is in m/s. The hydrogen generation rates plotted with respect to reciprocal temperature (1/K) is shown in Fig. 3.

From Fig. 3, the hydrogen production rate at 800 °C is $2.3 \cdot 10^{-3}$ liter/m^2/s, whereas that at 654 °C is $1.5 \cdot 10^{-4}$ liter/m^2/s, which is more than an order of magnitude smaller. For the tungsten rods which will be used for filling up the spallation volume inside the target wheel has a dimension of $3.0 \times 1.0 \times 8.0$ cm^3 has

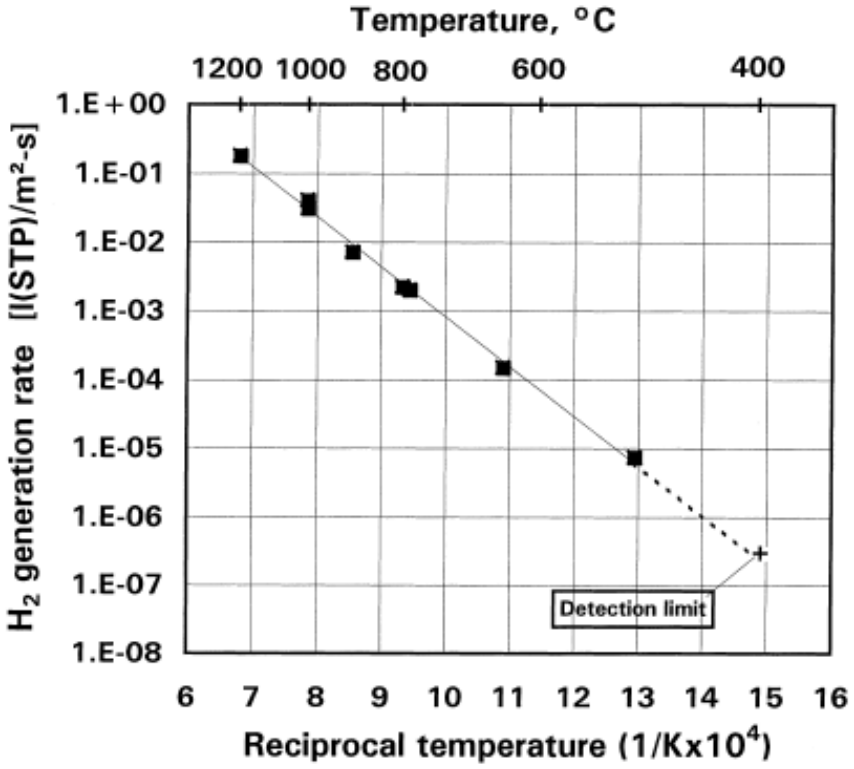

Figure 3: Hydrogen generation rates plotted with respect to reciprocal temperature (1/K) [9].

the surface area 70 cm^2. Assuming approximately 7000 tungsten rods will be used for filling up the spallation volume, the total surface area will be abour 50 m^2. Based on these numbers, a single target wheel will produce hydrogen gas at a rate of 0.12 liter/s at 800 °C and 0.008 liter/s at 654 °C, respectively.

In case that the maximum temperature of tungsten can be kept below 700 °C within the site boundary of ESS, the hydrogen partial pressure will reach the ignition point of 3.6 mol-% in 6 minutes in a confined volume of 1 m^3, assuming the hydrogen production rate of 0.1 liter/s. For reference, the maximum hydrogen generation rate in Ref. [9] is $1.86 \cdot 10^{-1}$ liter/m^2/s at 1200 °C, which amounts to the hydrogen generation rate of 9.3 liter/s from a target wheel. At this high temperature, the hydrogen partial pressure will reach the ignition point in 4 seconds in a confined volume of 1 m^3.

To conclude, it is important to keep the tungsten temperature below 700 °C within the site boundary of ESS in order to minimize the risk of hydrogen explosion due to tungsten oxidation. Below the temperature 700 °C, it will take hours until the concentration level of hydrogen generated from a target wheel reaches the ignition point, for instance, in a storage pit.

6 Pyrophoricity

Fine oxidisable tungsten powder mixed with air can constitute an explosion hazard, but the risk with tungsten powder is minimal with a self ignition temperature 310 °C [10].

The tungsten is classified as flammable solids category 1 (H228) according to GHS (Globally Harmonised System of Classification and Labelling of Chemicals [11]). The tungsten powder therefore should be kept away from heat, sparks, open flames and hot surfaces.

It has been reported in Ref. [12] that the tungsten powder with 1 μm average grain size could get ignited with a 2500 J electric discharge above minimum expressible concentration of 700 g·m^{-3}. The tungsten powder with average grain size 10 μm couldn't get ignited with a 2500 J electric discharge.

The source of tungsten dust at ESS should be the spallation target. The spallation volume will be made of pure tungsten which is either hot rolled or hot forged. The typical grain size of the powder metallurgically produced tungsten is larger than 10 μm, and the dust size which could come out from the operating tungsten target should be larger than 10 μm. For this reason, the risk of tungsten powder explosion hazard at ESS is not likely as the tungsten powder with average grain size larger than 10 μm is inflammable as referred above.

Regarding tungsten grain size, still the concern is that tungsten oxide powder which could be formed on the

spallation material surface in the target could have a tiny grain with the size smaller than 1 μm. But, tungsten trioxide is classified as inflammable solids according to GHS and it poses little concern in view of the explosion hazard risk at ESS.

7 Release of tungsten in normal operation via erosion

In normal operations, the erosion of tungsten by helium coolant flow is not expected, unless there is a surface micro-cracking failure due to cyclic thermal loads from beam trips and beam pulses. Particularly vulnerable to erosion could be oxidized tungsten surface, where the bonding of the tungsten oxide layer to the bulk tungsten should be weaker than the metallic bonding that holds tungsten together.

In this section, we estimate the release of tungsten to the helium cooling circuit of the target wheel due to erosion. The analysis is made in two parts, the contributions from the erosion of oxidized surface of tungsten and from the erosion of detached grains from the region of surface fracture failure.

7.1 Tungsten release via erosion of oxidized surface layer

In order to identify the erosion of tungsten oxide surface layer, an impinging helium jet experiment has been performed on a preoxidized tungsten specimen [13]. No quantifiable loss of tungsten oxide layer has been observed. Nevertheless, we will assume a total erosion of the tungsten oxide layer by the helium coolant flow in the tungsten release estimates below, for the sake of conservatism.

The tungsten blocks in the target wheel is exposed to oxygen impurity contents in the helium coolant. The physical parameters that are used for tungsten oxide erosion analysis is listed in Table 4.

Physical Parameter	**Mathematical Symbol**	**Unit**	**Description**
Total coolant mass	X	g	The filling mass of helium in the primary helium circuit
Oxygen fraction in X	Y	appm	The molar fraction of oxygen in the primary helium circuit
Filling rate	x	g/h	The filling rate of helium compensating the leak
Oxygen fraction in x	y	appm	The molar fraction of oxygen in the filling gas
Operation hour per year	H	hour	The annual target operation hour
Molar mass of helium	$\mathcal{M}_{He} = 4.00$	g/mol	Molar mass of helium
Molar mass of oxygen	$\mathcal{M}_{O_2} = 16.00$	g/mol	Molar mass of oxygen
Molar mass of tungsten	$\mathcal{M}_{W} = 168.84$	g/mol	Molar mass of tungsten
Molar mass of tungsten oxide	$\mathcal{M}_{WO_2} = 215.84$	g/mol	Molar mass of tungsten dioxide

Table 4: The physical parameters that are used for tungsten oxide erosion analysis.

We consider a situation where all the oxygen contents supplied to the primary helium cooling circuit is used for oxidizing the tungsten blocks in the target wheel and the tungsten oxide layer so formed is made of tungsten dioxide. In this case, the total molar quantity of oxygen that is used for oxidation per operational year is given by

$$\Lambda_{O_2} = 10^{-6} \cdot \frac{(X \cdot Y + x \cdot H \cdot y)}{\mathcal{M}_{He}} \quad [\text{mol}]. \tag{13}$$

The annual production of tungsten oxide layer in the target wheel is then given by the equation below,

$$M_{WO_2} = \mathcal{M}_{WO_2} \cdot \Lambda_{O_2} \quad [\text{g}]. \tag{14}$$

With a conservative assumption that all the tungsten oxide layer is eroded away by the helium flow, the total loss of tungsten per operational year is estimated by the equation below,

$$M_{W} = \mathcal{M}_{W} \cdot \Lambda_{O_2} \quad [\text{g}]. \tag{15}$$

For different oxygen impurity level, the annual production of tungsten loss from the target wheel is listed in Table 5.

Filling mass X [g]	**Filling rate** x [g/h]	O_2 **impurity** Y [appm]	O_2 **impurity** y [appm]	**Annual beam on target hours** [h]	**Annual W loss** [g/y]
$3.0 \cdot 10^4$	10.0	10.0	10.0	5400	38.6
$3.0 \cdot 10^4$	5.0	5.0	5.0	5400	13.1
$3.0 \cdot 10^4$	1.0	5.0	5.0	5400	8.14

Table 5: The annual production of tungsten loss from the target wheel.

In the absence of a helium purification system, the pure industrial helium typically has an oxygen impurity level of 5 appm, and the estimated leak rate of the primary cooling loop is 1 g/h. Under the ESS helium coolant loop conditions, the release of tungsten via the erosion of the oxide layer is estimated to be 10 g/year, even in the absence of purification system.

For reference, the tungsten erosion rate 10 g/year is amounts to average surface loss of 0.01 μm/year from the tungsten blocks. This number is considerably lower than the erosion rate of 10 μm/year assumed in the ESS Technical Design Report [14], that is due to the limited amount of oxigen impurities considered here but not taken into account in Ref. [14]. For reference, the erosion rate 0.01 μm/year in helium is comparable to the reported corrosion rate of 304 L stainless steel in water [15] within an order of magnitude. This indicates that the erosion rate of 10 g/year in innert helium flow is considered to be a conservative upper limit.

7.2 Tungsten release via erosion of surface crack

Due to thermal cycling induced by beam trips and beam pulses, surface fracture on the tungsten block might happen. This is particularly a concern because the operation temperature of the blocks will be in a brittle regime of tungsten with an onset of a radiation damage.

The crack formation on pure tungsten specimens under a high frequency of thermal cycling has been investigated in Ref. [16]. A high power electron beam was irradiated on actively cooled tungsten specimens of a dimension $12 \times 12 \times 5$ mm^3, with a beam spot size of 4×4 mm^2. The fatigue behavior of the tungsten surface has been investigated by applying a beam with pulse duration 0.48 ms and a repetition rate 25 Hz. Up to $1.0 \cdot 10^6$ number of pulses are applied, with varying power densities between 0.14 and 0.55 GW·m^{-2} on the beam spot area. Figure 4 shows the thermal fatigue curve presented in Ref. [16], where fatigue failure is defined by the formation of crack network on the surface and surface roughning. Note that the material showed no damage

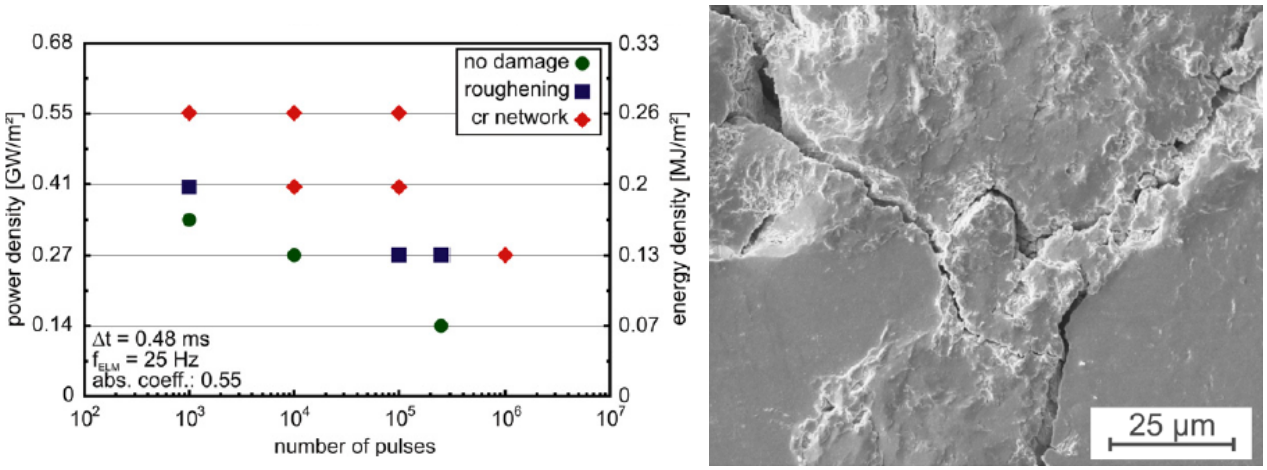

Figure 4: The thermal fatigue curve presented in Ref. [16](left) and the SEM image of the sample surface loaded with pulses of 0.27 GW·m^{-2} (right).

at the power density of 0.14 GW·m^{-2}. At this power density, a thermal and mechanical claculations are made by the author using ANSYS-Multiphysics tool, and the von Mises stress configuration is shown in Fig. 5. The calculated maximum stress on the surface of the thermal fatigue test specimen is 344 MPa at 0.14 GW·m^{-2}. This value is compared to the maximum stress in the tungsten blocks in the target wheel in Fig. 5, which is 96 MPa that is 28% of the thermal fatigue limit 344 MPa derived from the experimental result in Ref. [16].

The tungsten becomes brittle with proton irradiations, which could cause a degradation of the mechanical strength and the fatigue limit. So far, there is no solid data on the radiation induced tungsten damages

regading thermal fatigue properties. The preliminary results from the PIE of STIP-V tungsten specimens with a comparable proton and neutron damages to the ones expected in ESS target operation indicate that the UTS of tungsten degrades to about 50% of the unirradiated value. Even taking 70% margin from the fatigue limit of 344 MPa, the maximum stress of the tungsten blocks in the target wheel still stays below the conservatively adjusted fatigue limit of 100 MPa. Therefore, it is highly unlikely that erosion of the tungsten surface would happen by the helium coolant flow, caused by the dust created from the tungsten surface cracks.

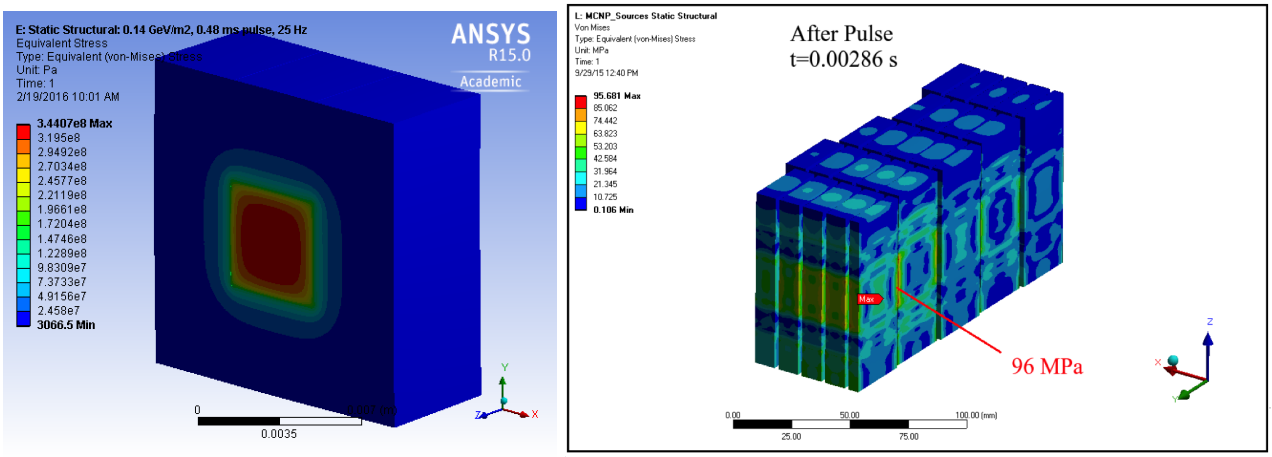

Figure 5: The calculated von Mises stress profiles in the tungsten specimen used for the thermal fatigue experiments in Ref. [16] (left) and in the tungsten blocks in the target wheel (right), at the crest of each beam pulse.

7.3 Total tungsten release during annual operation

To summarize, the total loss of tungsten due to erosion by the helium coolant flow is estimated to be maximum 10 g/year, which is mainly due to the total loss of tungsten oxide layer.

8 Release of tungsten in a severe accident - Target wheel stopping and beam on

During accidents where the tungsten temperature becomes above 700 °C, the tungsten mass from the wheel can be released via oxidation of tungsten followed by evaporation of oxidized layer. In this section, we consider a severe accident case where the target wheel accidentally stops and the 5 MW proton beam continues to shoot the same target segment with a repetition rate of 14 Hz.

Assuming adiabatic heating of the tungsten blocks during beam pulses, the maximum temperature in the tungsten block increases as given in Table 6. The post-pulse temperatures will be used as a reference in the hazard analysis presented below.

8.1 Case - Intact helium or vacuum environment in the monolith

8.1.1 Tungsten sublimation

In the absence of oxygen or vapour, the tungsten blocks will not get oxidized. Instead, the tungsten blocks could sublimate in case the unstopped beam over-heats the affected target segments. Maximum particle flux Φ_W from a tungsten block sublimation is obtained when the ambient pressure is assumed to be absolute zero. The equation for the maximum particle flux can be derived from kinetic theory,

$$\Phi_W = 3.513 \cdot 10^{22} \frac{P_W}{\sqrt{\mathcal{M}_W T}} \quad [\ \text{molecules}\cdot\text{cm}^{-2}\cdot\text{s}^{-1}\ ], \tag{16}$$

$$= 5.84 \cdot 10^{-2} \sqrt{\frac{\mathcal{M}_W}{T}}\, P_W \quad [\ \text{g}\cdot\text{cm}^{-2}\cdot\text{s}^{-1}\ ], \tag{17}$$

as a function of tungsten vapor pressure P_W and the surface temperature. Here, $\mathcal{M}_W$ is molecular weight of tungsten in [g/mol], T is surface temperature in [K] and P_W is vapor pressure of pure tungsten in [torr].

Pulse number	**Pre-pulse temperature [K]**	**Specific heat at pre-pulse [J·g^{-1}·K^{-1}]**	**Temperature amplitude [K]**	**Post-pulse temperature [K]**
Pulse 01	650.00	0.140	105.60	755.60
Pulse 02	755.60	0.143	103.28	858.88
Pulse 03	858.88	0.146	101.15	960.03
Pulse 04	960.03	0.149	99.20	1059.23
Pulse 05	1059.23	0.152	97.40	1156.63
Pulse 06	1156.63	0.155	95.74	1252.37
Pulse 07	1252.37	0.157	94.20	1346.56
Pulse 08	1346.56	0.160	92.76	1439.33
Pulse 09	1439.33	0.162	91.43	1530.75
Pulse 10	1530.75	0.164	90.18	1620.93
Pulse 11	1620.93	0.166	89.01	1709.93
Pulse 12	1709.93	0.168	87.91	1797.85
Pulse 13	1797.85	0.170	86.88	1884.73
Pulse 14	1884.73	0.172	85.91	1970.64
Pulse 15	1970.64	0.174	85.00	2055.64
Pulse 16	2055.64	0.176	84.14	2139.78
Pulse 17	2139.78	0.178	83.33	2223.11
Pulse 18	2223.11	0.179	82.56	2305.68
Pulse 19	2305.68	0.181	81.84	2387.52
Pulse 20	2387.52	0.182	81.15	2468.67
Pulse 21	2468.67	0.184	80.51	2549.18
Pulse 22	2549.18	0.185	79.89	2629.07
Pulse 23	2629.07	0.187	79.31	2708.38
Pulse 24	2708.38	0.188	78.76	2787.14
Pulse 25	2787.14	0.189	78.24	2865.38
Pulse 26	2865.38	0.190	77.74	2943.12
Pulse 27	2943.12	0.192	77.27	3020.40
Pulse 28	3020.40	0.193	76.83	3097.23

Table 6: The analytic estimates of maximum temperature in the tungsten block before and after each pulse, assuming adiabatic heating during accident.

The enthalpy of tungsten evaporation and the temperature dependent tungsten vapor pressure are presented in Ref. [17] in the temperature range 2600 to 3100 K,

$$\log P_W \text{ [atmosphere]} = -\frac{45385}{T} + 7.871 \quad (18)$$

$$\log P_W \text{ [torr]} = -\frac{45385}{T} + 10.752 \quad (19)$$

$$\Delta H = 859.90 \pm 4.6 \quad \text{kJ·mol}^{-1}. \quad (20)$$

Table 7 lists the calculated values for the tungsten evaporation rate from a single tungsten block for chosen temperatures. Here, we assumed the total surface area of 70 cm^2 for a tungsten block. If the target wheel

Temperature [**K**]	P_W [**torr**]	Φ_W [**g·cm^{-2}·s^{-1}**]	Φ_W [**g·block^{-1}·s^{-1}**]	**Time to complete sublimation** [s]
2600	$1.98 \cdot 10^{-7}$	$3.07 \cdot 10^{-9}$	$9.34 \cdot 10^{-7}$	$2.16 \cdot 10^{9}$
2700	$8.76 \cdot 10^{-7}$	$1.34 \cdot 10^{-8}$	$3.66 \cdot 10^{-6}$	$4.96 \cdot 10^{8}$
2800	$3.49 \cdot 10^{-6}$	$5.22 \cdot 10^{-8}$	$1.30 \cdot 10^{-5}$	$1.27 \cdot 10^{8}$
2900	$1.26 \cdot 10^{-5}$	$1.86 \cdot 10^{-7}$	$4.25 \cdot 10^{-5}$	$3.56 \cdot 10^{7}$
3000	$4.20 \cdot 10^{-5}$	$6.08 \cdot 10^{-7}$	$1.29 \cdot 10^{-4}$	$1.09 \cdot 10^{7}$
3100	$1.29 \cdot 10^{-4}$	$1.84 \cdot 10^{-6}$	$3.63 \cdot 10^{-4}$	$3.60 \cdot 10^{6}$

Table 7: The calculated values for the tungsten evaporation rate from a single tungsten block for chosen temperatures. Here, we assumed the total surface area of 70 cm^2 for a tungsten block.

stops while beam is on, the maximum temperature in the affected segment will rise to 3100 K after about 28 pulses. Conservatively assuming a uniform temperature of 3100 K in a target segment, which contains about 200 tungsten blocks, the total tungsten sublimation rate becomes 25.7 μg·s^{-1}. If the beam is stopped after 28 pulses, and the uniform temperature level of 3100 K in the affected segment is held for 1 hour, the amount of tungsten that is vaporized in the monolith atmosphere is estimated to be 93 grams, which is about 0.003% of total tungsten mass in the target wheel.

8.1.2 Radioinventory diffusion

When released from tungsten, among other istopes produced in tungsten, the Gd-148 and the Hf-172 accounts for 80% of total radiation dose to the surroundings [18]. In case of accidents, where the temperature in the tungsten blocks excurses to a high temperature, the diffusion release of these isotopes will account for the radiation dose in the monolith to a large fraction.

The diffusion constants of Gd and Hf are given by Arrhenius equation,

$$D = D_0 \exp\left(-\frac{E_A}{kT}\right), \quad (21)$$

where E_A is an activation energy, D_0 is a pre-exponential factor, $k = 8.61734 \cdot 10^{-5}$ eV·K^{-1} is a Boltzmann constant and T is the absolute temperature. The material specific values for D_0 and E_A are compiled in Ref. [19] for selected isotopes, which include Gd and Hf. Once the diffusion constants are known, the diffusion driven

Element	D_0 [**cm^2·s^{-1}**]	E_A [**eV**]
Gd	0.195	4.83
Hf	2.19	5.78

Table 8: The material specific values for D_0 and E_A for Gd and Hf.

release fraction f_d from a d cm thick tungsten slab can be calculated by

$$f_d \simeq 2.281\sqrt{\frac{Dt}{d^2}}, \quad \text{for } \tfrac{Dt}{d^2} \ll 1, \quad (22)$$

where t is time in [s].

We consider an accidental case, where the target wheel stops and the beam is on before it is stopped by a intervention of Target Safety System. Table 9 lists the calculated values for the the release fractions f_d of Gd and Hf from a 1 cm thick tungsten block, if the given temperature is kept in the tungsten block for 1 hour after the accident. For the type of accident considered here, the total release factor of radio isotopes should be less

Temperature [K]	**f_d for Gd at given temperature for 1 hour**	**f_d for Hf at given temperature for 1 hour**
300	1.63E-39	5.71E-47
400	2.26E-29	7.84E-35
500	2.75E-23	1.50E-27
600	3.13E-19	1.08E-22
700	2.48E-16	3.16E-19
800	3.69E-14	1.26E-16
900	1.81E-12	1.33E-14
1000	4.08E-11	5.52E-13
1100	5.21E-10	1.16E-11
1200	4.35E-09	1.48E-10
1300	2.62E-08	1.27E-09
1400	1.22E-07	8.00E-09
1500	4.65E-07	3.95E-08
1600	1.49E-06	1.60E-07
1700	4.19E-06	5.48E-07
1800	1.05E-05	1.64E-06
1900	2.37E-05	4.37E-06
2000	4.96E-05	1.06E-05
2100	9.67E-05	2.35E-05
2200	1.77E-04	4.85E-05
2300	3.09E-04	9.42E-05
2400	5.13E-04	1.73E-04
2500	8.18E-04	3.02E-04
2600	1.26E-03	5.07E-04
2700	1.88E-03	8.17E-04
2800	2.72E-03	1.27E-03
2900	3.84E-03	1.92E-03
3000	5.30E-03	2.83E-03
3100	7.16E-03	4.06E-03

Table 9: The calculated diffusion release fraction of Gd and Hf from tungsten blocks that are kept at given temperatures 1 hour.

than 0.1% even at 3100 K.

8.2 Case - Breach of monolith environment and ingress of water into the target area

An accidental situation is considered, where the target wheel is stopped with beam-on, the target vessel loses helium coolant confinement and the top pre-moderator vessel is broken, leaking water onto the target shroud. In this scenario, the leaked water from the pre-moderator will be boiled by heated target segment and the monolith atmosphere is filled with steam. If the heated tungsten blocks with temperature higher than 700 °C, the steam first oxidize the tungsten surface to WO_3 and then hydrate it to H_2WO_4 and evaporating the tungsten hydrate [7, 20].

For reference, the heat of vaporization of water is 40.66 kJ/mol or 2.257 MJ/kg. If 60% of the beam power is used to evaporate water that leaks from the top pre-moderator, about 100 g (5.3 mol) of steam per single pulse will be generated. If all of the generated steam is used for oxidizing the tungsten surface to WO_3, about 323 g (1.76 mol) of tungsten per single proton pulse will be evaporated. For reference, if the TSS intervenes to stop the beam in 30 pulses, up to 9 kg (about 0.1% of total tungsten fraction in the target wheel) of tungsten could be released to the monolith vessel volume, assuming an extreme situation where the steam is uniformly distributed in the target wheel.

The empirical fit for the vaporization rate of tungsten in 100% steam is presented in Ref. [20],

$$\dot{M}_W \text{ g·cm}^{-2}\text{·s}^{-1} = A \exp\left(-\frac{\Delta H}{RT}\right) = 2611 \exp\left(-\frac{48900}{RT}\right), \tag{23}$$

where $\dot{M}_W$ is the rate of tungsten-metal vaporized per unit surface area, $\Delta H = 48.9$ kcal·g-mol^{-1} is the heat of vaporization, $R = 1.987$ cal·g-mol^{-1}·K^{-1} is the gas constant, and T is the tungsten surface temperature in [K]. It is not likely that the tungsten blocks in the affected target segment are in 100 % steam atmosphere. But

Temperature [K]	$\dot{M}_W$ **[g·cm^{-2}·s^{-1}]**	$\dot{M}_W$ **[g·block^{-1}·s^{-1}]**	**Time to complete evaporation [s]**
800	1.14E-10	7.98E-09	5.81E+10
900	3.48E-09	2.43E-07	1.90E+09
1000	5.36E-08	3.75E-06	1.24E+08
1100	5.02E-07	3.51E-05	1.32E+07
1200	3.24E-06	2.27E-04	2.04E+06
1300	1.57E-05	1.10E-03	4.22E+05
1400	6.06E-05	4.24E-03	1.09E+05
1500	1.96E-04	1.37E-02	3.38E+04
1600	5.46E-04	3.82E-02	1.21E+04
1700	1.35E-03	9.44E-02	4.91E+03
1800	3.01E-03	2.11E-01	2.20E+03
1900	6.19E-03	4.33E-01	1.07E+03
2000	1.18E-02	8.28E-01	5.60E+02
2100	2.12E-02	1.49E+00	3.11E+02
2200	3.62E-02	2.53E+00	1.83E+02
2300	5.89E-02	4.12E+00	1.12E+02
2400	9.19E-02	6.44E+00	7.20E+01
2500	1.39E-01	9.70E+00	4.78E+01
2600	2.02E-01	1.42E+01	3.27E+01
2700	2.87E-01	2.01E+01	2.30E+01
2800	3.98E-01	2.78E+01	1.66E+01
2900	5.39E-01	3.77E+01	1.23E+01
3000	7.15E-01	5.00E+01	9.26E+00

Table 10: The calculated values for the tungsten evaporation rate from a single tungsten block for chosen temperatures in 100% steam atmosphere. Here, we assumed the total surface area of 70 cm^2 for a tungsten block.

if we assume that the generated steam spreads ideally in the target wheel to provide an ideal condition for the tungsten oxidization, a tungsten block will be evaporized completely in 10 minutes for the temperature above 2000 K. At this temperature, maximum amount of tungsten that can be lost is 9 kg, as stated above.

The hydrogen generation becomes an issue at high temperature. For reference, the maximum hydrogen generation rate in Ref. [9] is $1.86 \cdot 10^{-1}$ liter/m^2/s at 1200 °C, which amounts to the hydrogen generation rate of 0.26 liter/s from the affected target wheel segment. At this high temperature, the hydrogen partial pressure will reach the ignition point in the monolith vessel volume of about 10 m^3 in about half an hour, in an extreme conditions with the presence of a enough amount of air or dissosiated oxygen atmosphere in the monolith vessel.

References

[1] H. Ullmaier and F. Carsughi. Radiation damage problems in high power spallation neutron sources. *Nuclear Instruments and Methods in Physics Research B*, 101:406–421, 1995.

[2] Michael Rieth, Andreas Hoffmann, Edeltraud Materna-Morris, and Magnus Rohde. Tungsten materials for structural divertor applications. Technical Report http://bibliothek.fzk.de/zb/veroeff/80215.pdf, KIT.

[3] J. Habainy, S. Iyengar, Y. Lee, and Y. Dai. Fatigue behavior of rolled and forged tungsten at 25°, 280° and 480°. *Journal of Nuclear Materials*, 2015.

[4] ITER EDA. ITER Material Properties Handbook. Technical Report ITER Document No. S 74 MA 2, ITER, June 1998.

[5] J. Habainy, C. Nilsson, J. Wendel, S. Iyengar, Y. Lee, and Y. Dai. Oxidation behaviour of pure tungsten in mildly oxidizing atmospheres. In *12th International Workshop on Spallation Materials Technology*, 19-23 October 2014 Bregenz, Austria.

[6] F. Druyts, J. Fays, and C. H. Wu. Interaction of plasma-facing materials with air and steam. *Fusion Engineering and Design*, 63-64:319–325, 2002.

[7] G. A. Greene and C. C. Finfrock. Vaporization of tungsten in flowing steam at high temperatures. *Experimental Thermal and Fluid Science*, 25:87–99, 2001.

[8] S. C. Cifuentes, M. a. Monge, and P. Pérez. On the oxidation mechanism of pure tungsten in the temperature range 600-800 °C. *Corrosion Science*, 57:114–121, 2012.

[9] G.R Smolik, K.a McCarthy, D.a Petti, and K Coates. Hydrogen generation from steam reaction with tungsten. *Journal of Nuclear Materials*, 258-263:1979–1984, 1998.

[10] Oleg D. Neikov, I. B. Murashova, Nicholas A. Yefimov, and Stanislav Naboychenko. *Handbook of Non-Ferrous Metal Powders: Technologies and Applications*. Number ISBN: 978-1-85617-422-0. Elsevier, 2009.

[11] *Globally Harmonised System of Classification and Labelling of Chemicals*. United Nations, fourth revised edition edition, 2011.

[12] Kenneth L. Cashdollar and Isaac A. Zlochower. Explosion temperatures and pressures of metals and other elemental dust clouds. *Journal of Loss Prevention in the Process Industries*, 4(20):337–348, July 2007.

[13] Per Nilsson. ETHEL Erosion Tests. Technical Report ESS-0051445, European Spallation Source ERIC, 2016.

[14] S. Peggs and R. Kreier, editors. *ESS Technical Design Report*. Number ISBN 978-91-980173-2-8 in ESS-doc-274. April 2013.

[15] P. L. Rittenhouse, S. A. Maloy, and M. W. Cappiello. Afci materials handbook: Materials data for particle accelerator applications. Technical Report LA-CP-06-0904 - Revision 5, Los Alamos National Laboratory, June 2006.

[16] Th Loewenhoff, a Bürger, J Linke, G Pintsuk, a Schmidt, L Singheiser, and C Thomser. Evolution of tungsten degradation under combined high cycle edge-localized mode and steady-state heat loads. *Physica Scripta*, T145:014057, 2011.

[17] E. R. Plante and A. B. Sessoms. Vapor Pressure and Heat of Sublimation of Tungsten. *JOURNAL OF RESEARCH of the National Bureau of Standards-A. Physics and Chemistry*, 77A(2):237–242, March-April 1973.

[18] Jens Harborn. Radiological Hazard Accident Scenario Analysis Target Helium cooling systems. Technical Report ESS-0039961, European Spallation Source ERIC, 2016.

[19] Eric Pitcher. Elemental Release from the ESS Tungsten Target During Normal Operation. Technical Report ESS-0044391, European Spallation Source ERIC, 2016.

[20] G. A. Greene, C. C. Finfrock, and A. L. Hanson. Behavior of High-Temperature Tungsten and Inconel in Spallation Target Applications. In *Accelerator Applications in a Nuclear Renaissance (AccApp 2003)*, June 2003.